Research Article | Vol. 27, No. 9 | 29 Apr 2019 | OPTICS EXPRESS 13061
Optics EXPRESS

Two-dimensional liquid crystal polarization grating via linearly polarized light modified multi-beam polarization interferometry

YUE SHI,[1] YINGMING LAI,[1] YAN JUN LIU,[1] VLADIMIR G. CHIGRINOV,[2] HOI-SING KWOK,[2] MINGGANG HU,[3] DAN LUO,[1,*] AND XIAO WEI SUN[1]

[1]*Department of Electrical and Electronic Engineering, Southern University of Science and Technology, No. 1088, Xueyuan Rd., Xili, Nanshan District, Shenzhen, Guangdong 518055, China*
[2]*State Key Laboratory on Advanced Displays and Optoelectronics Technologies, Department of Electronic and Computer Engineering, The Hong Kong University of Science and Technology, Clear Water Bay, Kowloon, Hong Kong, China*
[3]*Xi'an Modern Chemistry Research Institute, Xi'an, Shanxi 710065, China*
**luo.d@sustc.edu.cn*

Abstract: Holographic lithography is widely used as an effective approach for two-dimensional (2D) photonic crystal fabrication. However, for the fabrication of 2D polarization structures based on photoaligned liquid crystals (LCs), holographic lithography method is limited. The fabrication requires full coverage of light intensity, 2D chiral distribution and continuously varying polarization direction, which could be hardly guaranteed by multi-beam interference of circularly polarized light (CPL). Herein, we introduce a linearly polarized light (LPL) into a three-CPL interference configuration to improve the interference field and fulfill the critical requirement. The introduced LPL intensity is chosen to be 1/5 of the CPL to guarantee both full coverage of light intensity and well photoalignment defined LC directors. Moreover, the introduction of the weak LPL into multiple CPL interference is shown to give little disturbance to the desired diffraction properties.

1. Introduction

Light polarization, as another light parameter besides intensity and phase, has attracted intensive attention [1–3]. Efficient control of light polarization is of particular importance for various applications, such as imaging, display, optical communications and so on [1–5]. In particular, polarization grating (PG) shows great potentiality for beam splitting, polarization conversion and beam steering applications [6–10]. Studies show that two orthogonally polarized CPL interference gives a uniform intensity and one-dimensional (1D) periodically varying linear polarization distribution [6,7]. This polarization modulation can be recorded by polarization-sensitive materials [11–14] and transferred to LC to give a 1D PG. The continuous LC director distribution locally modifies the polarization state of light, so that it has the polarization selective diffraction property and could reach 100% diffraction efficiency on the first order at half-wave condition [7]. Therefore, the 1D PG has attracted intensive attention and been studied extensively [8–10].

However, there were only limited reports of 2D PGs, which could be fabricated either by superposition of two 1D PGs [15,16], or through multi-beam polarization interference [17–20]. For the first kind of 2D PGs, the structure design is limited. For the second kind of 2D PGs, the polarization structure and diffraction pattern should have rich diversity and be more attractive. However, different from the traditional multi-beam holographic lithography which has been widely used for the 2D binary grating and photonic crystal/quasicrystal fabrications [21–23], the requirement for 2D polarization structure realization is much more critical [24]. Firstly, the null intensity area should be avoided in the interference field, or else the

#360038 https://doi.org/10.1364/OE.27.013061
Journal © 2019 Received 12 Feb 2019; revised 3 Apr 2019; accepted 9 Apr 2019; published 24 Apr 2019

photosensitive materials cannot be completely oriented [19,20]. Secondly, the polarization direction should have 2D chiral distribution and vary continuously in the whole area, which is required for 2D PG to give high efficient and polarization selective diffraction. The continuous polarization direction distribution is also required by LC material due to the energy minimization requirement [25]. Otherwise, the LC directors cannot follow the desired polarization distribution, and defects and undefined orientations at the sudden-change area will occur. Therefore, the interference configuration should be carefully selected or modified for both the intensity and polarization direction distribution requirements. However, almost all the previous studies didn't consider both requirements simultaneously, and only poor 2D diffraction properties were demonstrated [17–20]. In our recent study, we explored the multi-CPL interference field and found that the interference of four CPL with RCP-RCP-LCP-RCP configuration (RCP: right circularly polarized; LCP: left circularly polarized) could satisfy both requirements, and a 2D PG with high diffraction efficiency and polarization selectivity has been demonstrated [24]. However, only limited 2D PGs could be obtained through this method since the two conditions could be hardly satisfied at the same time based on simulation results, which we have tested from three-beam to nine-beam interference.

Herein, we found that the polarization distribution of multi-CPL-interference field could be modified by introducing a weak LPL into the interferometry. For example, the polarization orientations of the three-CPL interference field have sudden changes. However, by introducing a weak LPL intoa fourth arm, the polarization distribution could be modified, making the polarization direction to be more continuous. Using weak LPL modified multi-CPL polarization interferometry, the obtained 2D liquid crystal polarization grating (LCPG) has similar diffraction property as expected for the multi-CPL case as long as the added beam stays weak. The diffraction keeps high efficiency, polarization selective and good diffracted CPLquality with orthogonal polarizations. Our proposal may provide another perspective to overcome the critical requirement for 2D polarization structure fabrication, and may be extended to sub-micron scale to provide an effective way for polarization photonic crystal fabrication.

2. Simulation and experimental

The simulation was done through Matlab. The electric vector of each interferential beam can be expressed as $\vec{E}_i = A_i \hat{p}_i \exp\{i\vec{k}_i \cdot \vec{r}\}$, where A_i is the amplitude and $\hat{p}_i$ is the polarization vector. The propagation vector is $\vec{k}_i = k[-\sin\theta_i, 0]$, where $k = 2\pi / \lambda$. The light interference on the *x*-*y* plane can be calculated as $\vec{E}(x,y) = \sum_{i=1}^{4} \vec{E}_i(x,y)$ and $I(x,y) = \left|\vec{E}(x,y)\right|^2$ for the electric field and intensity distribution respectively. To obtain the polarization distribution, the electric vector can be expressed as a general form of elliptically polarized light (EPL) $\vec{E}(x,y) = (A_x e^{i\delta_x}, A_y e^{i\delta_y})^T$, where the polarization ellipticity, orientation and helicity can be fully characterized [26]. The ellipticity is the ratio of minor to major axis of polarization ellipse $\mp b/a = \tan\chi$, where χ is the ellipticity angle determined by $\sin 2\chi = -2\,\mathrm{Im}[\gamma]/(1+|\gamma|^2)$. The polarization orientation can be expressed by angle ψ: $\tan 2\psi = 2\,\mathrm{Re}[\gamma]/(1-|\gamma|^2)$, where the auxiliary parameter is $\gamma = A_y e^{i\delta_y} / A_x e^{i\delta_x} = A_{yx} e^{i\delta}$. The helicity of the ellipse can be indicated either by the sign of angle χ or δ. If either one is positive, the light is right-handed polarized. If either one is negative, the light is left-handed polarized. In particular, when $\chi = \pm\pi/4$, it is CPL; when $\chi = 0$, the EPL degenerates to LPL.

The interference setup was built based on a 488 nm Ar^+ laser with long coherence length on a floated optical table. The four beams converged symmetrically along the orthogonal planes with the same polar angle θ (~2.4°) using beam splitters in symmetric arrangement. A

pair of polarizer and quarter-wave plate (QWP) was put in three arms to generate CP light, and another polarizer was used in the other arm to get LP light. To control the light intensity of each beam, a half-wave plate (HWP) was applied before each polarizer. During the light interference experiments, the CPL intensity was kept at 16 mW/cm^2 each, while the LPL intensity was adjustable and the recording time varied from 3 to 10 minutes correspondingly.

An azobenzene sulfonic dye SD1 (DIC Inc.) was used for interference pattern recording [27].The SD1 material was dissolved in N,N-dimethylformamide (DMF) at a concentration of 1 wt% to spin-coat on a substrate, and followed by soft-baking at 100 °C for 10 min for solvent evaporation. After interference light exposure, the polarization orientation was recorded by the photoalignment layer. Then a layer of LC polymer UCL017 (DIC Inc., Δn = 0.17) was spin-coated on top. The LC directors would follow the director distribution of SD1 molecules due to the anisotropic anchoring effect. An additional deep UV polymerization was used to fix the LC director to make it a solid film, where the deep UV could not disturb the patterned alignment. In this process, the LC polymer thickness could be adjusted by solution concentration, coating speed, or using multiple LC polymer layers. On the other hand, to fabricate a tunable 2D LCPG, a 2 μm-thick ITO glass cell with SD1 inter coating on both substrates was used. A nematic LC material HM2 with high birefringence Δn = 0.37 was filled into the photo-patterned cell by capillary action [28]. The local transmitted light intensity of LC under polarized optical microscopy (POM) is $I = I_0 \sin^2(2\varphi)\sin^2(\pi\Delta nd/\lambda)$, where Δnd is the LC phase retardation and φ is the azimuthal angle.

The diffraction property of the 2D PG fabricated by LC polymer was investigated by the different probing beams and polymer thicknesses to get different phase retardations. For the LC cell investigation, a632.8 nm He-Ne probing laser was used to avoid pattern erasing, and a sinusoidal ac voltage was applied to adjust the LC phase retardation. The probe beam was LP in general, which could be changed to LCP or RCP by a QWP with its fast axis + 45° or –45° to the polarization direction. The polarization ellipticity of the diffracted light was characterized by a rotating polarizer. The helicity was checked by a QWP and a polarizer with the polarization axis + 45° or –45° to the fast axis of the QWP based on Jones calculus. For diffraction simulation, Fourier transform was applied for the transmitted electric field through the LCPG where $\vec{E}_{out}(x,y) = T(x,y)\vec{E}_{in}$. $T(x,y) = R[-\varphi(x,y)]T_{WP}R[\varphi(x,y)]$ is the transfer matrix of a LC wave plate T_{WP} with spatially varying director field $\varphi(x,y)$, and $R[\varphi(x,y)]$ is the rotation matrix.

3. Results and discussion

For multi-beam interference method for 2D LC polarization structure fabrication, two conditions need to be satisfied using photosensitive materials [24]. Firstly, null intensity area should be avoided, so that the photosensitive material could be photo induced all over the interference area. Secondly, the polarization direction should have 2D chiral distribution and vary continuously in the whole area, so that it can be fully transferred to LCs using photoalignment method. If there is a sudden change in the polarization orientation, random orientations and defects may be induced, and the expected polarization structure and diffraction property can be hardly obtained.

Figure 1 shows the simulation result of three-CPL interference. Although the light intensity covers the whole area [Fig. 1(b)], the polarization directions have sudden changes in *y*-direction, which is realized by gradually changing ellipticity as shown in Fig. 1(c). Let we neglect the elastic energy requirement of LC material first and assume the LC directors could be completely aligned perpendicularly to the long axis of the polarization ellipses and the ideal 2D polarization structure could be well obtained. Four 1st order scattered spots with polarization selectivity are expected as shown in Figs. 1(e) and 1(f). This diffraction property will be used for comparison with the modified case later. However, due to the elastic requirement of LC material, LC directors cannot follow the sudden change of polarization

Optics EXPRESS

directions, and therefore the fabrication of photo-aligned 2D polarization structure based on this interference configuration is not feasible.

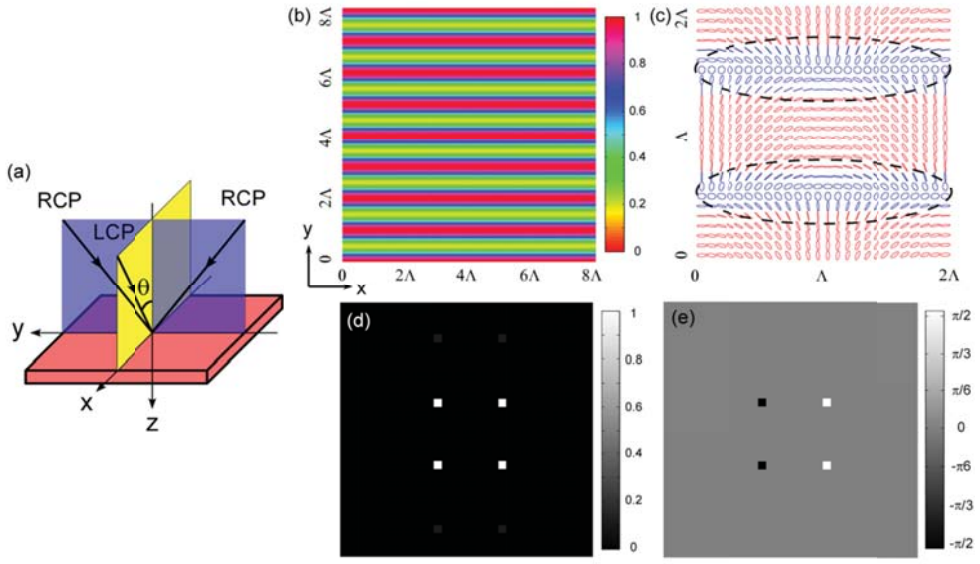

Fig. 1. Simulation results of three-CPL interference. (a) Schematic diagram of the three-beam arrangement. (b) Intensity and(c) polarization distribution of the interference field, where $\Lambda = \lambda / 2\sin\theta$. The black dashed ellipses indicate the areas where the directions of polarization ellipses have 90° sudden change in *y*-direction. Different colors indicate different polarization states. Blue: left-handed polarization; Red: right-handed polarization. (d) Diffraction of the ideal 2D LCPG at half-wave condition. (f) Phase of the main diffracted beams.

In an attempt to avoid the aforementioned obstacles, another beam is introduced to modify the interference pattern. As shown in Fig. 2(a), we add a LP beam into the interference configuration, where the four beams converge symmetrically along the orthogonal planes with the same incident angle. The intensity distribution varies with the introduced LPL intensity, where the intensity ratio between I_{max} and I_{min} is plotted in Fig. 2(b). We can see that no null intensity area will be caused. On the other hand, the polarization distribution can be modified by the introduction of LPL. As shown in Figs. 2(c) and 2(d), the polarization directiondistribution becomes more continuous as the introduced LPL intensity increasing compared to Fig. 1(c). Therefore, the introduction of a LP beam may help to modify the polarization interference field of CPL to overcome the critical requirement for 2D polarization structure fabrication.

A photoalignment material SD1 is used for polarization information recording. When exposed to LPL, azobenezene molecules are aligned perpendicularly to the polarization direction [29]. If the excitation is EPL, the azobenzene molecules will be aligned perpendicularly to the long axis of polarization ellipse [30]. Azobenzene material SD1 is chosen because it has been proven to have good thermal stability and strong anchoring strength for applications on various LC photonic devices [31,32]. Its anchoring strength increases with light exposure, and becomes saturated with stronger illumination [14,33], while the layer morphology do not change with the excitation dosage. Therefore, although the light intensity is not uniform, as long as there is no null intensity area, the SD1 molecules will be fully reoriented by extended photo excitation.

Optics EXPRESS

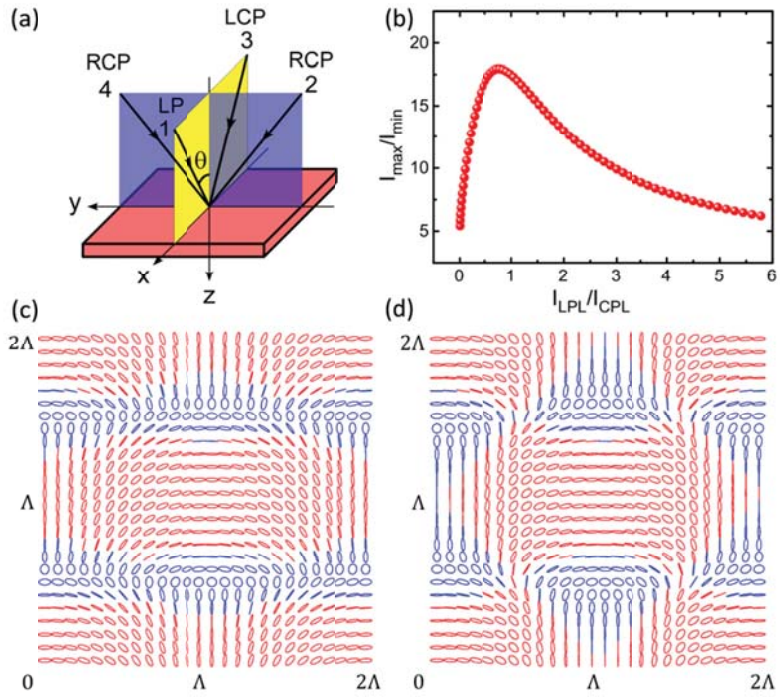

Fig. 2. Simulation results of light interference by introducing a LP beam. (a) Schematic diagram of the beam arrangement. (b) Intensity ratio I_{max}/ I_{min} of the interference field varies with the intensity ratio of LPL and CPL.Polarization distribution of the interference field when (c) $I_{LPL} = I_{CPL}/5$, and (d) $I_{LPL} = I_{CPL}$.

From experiments, we find that the LC texture does improve with increasing light intensity of the introduced LPL, since the continuity of the polarization direction gets better as expected from simulation. When the LPL intensity increases to 1/5 of the CPL, the LC texture could be fully identified. The LC texture from simulation is shown in Figs. 3(a) and 3(b), where the LC directors are assumed to be perpendicularly to the polarization direction. The experimental LC texture shows some deviation compared to the simulation result due to the elastic energy minimization requirement of LC material [Fig. 3(c)]. Although the ± 45° oriented areas expand and the vertically aligned areas shrink, the self-modified LC directors give fully identified LC texture. If the LPL intensity further increases, the polarization continuity will be further improved and the LC texture gets better identified and becomes more consistent with the simulation results. However, higher LPL intensity will cause diffraction issue and thus should be avoided, which will be discussed later in detail.

The diffraction of the designed 2D LCPG is analyzed and shown in Fig. 4. The incident beam is mainly diffracted into four spots on the 1st order, similar to that of the three CPL interference case as shown in Fig. 1(d). However, there are two additional diffraction spots marked as the 2nd order in Fig. 4(a), which are caused by the polarization modification due to LPL introduction. It will stay weak as long as the introduced LPL intensity is low based on simulation. The diffraction efficiency of the 2D LCPG varies with the LC phase retardation as expected for PG, where those of the first three orders are plotted in Fig. 4(b). The maximum diffraction happens at half-wave condition, where the1st order occupies about 77% of the total energy obtained from simulation. As the introduced LPL intensity increases, the diffraction to both 0th and 2nd orders become more obvious and the diffraction efficiency of the 1st order will decrease, and thus high LPL intensity in the interferometry should be avoided.

Optics EXPRESS

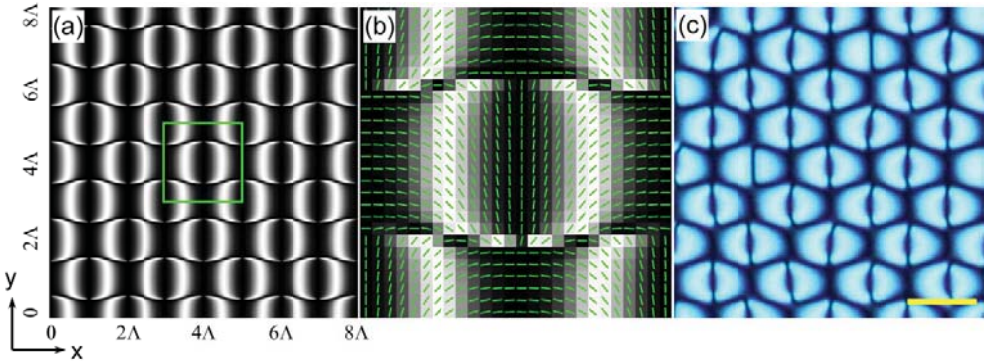

Fig. 3. 2D LC texture under POM when $I_{LPL} = I_{CPL}/5$.(a) Simulated LC texture. (b) Simulated LC texture with director configuration (green short lines) in one period. (c) LC texture realized experimentally. The scale bar is 10 μm.

Figure 4(c) shows the diffraction of a fabricated 2D LCPG with $I_{LPL} = I_{CPL}/5$at about the half-wave condition (LC polymer thickness~1.59 μm).The measured diffraction efficiencies of the 0th and 1st orders at different phase retardations are shown in Fig. 4(b). The experimental data basically follow the simulation results. The discrepancies, for example, the 1st order diffraction efficiency is not as high as simulation, are mainly due to the small optical misalignment of the multi-beam interference setup, which is hard to be completely avoided in our experiments by hand adjustment. The misalignment could reduce the 1st order diffraction efficiency and makes the 0th order more obvious. In addition, the scattering from non-perfectly aligned LC polymer could also decrease the total diffraction efficiency.

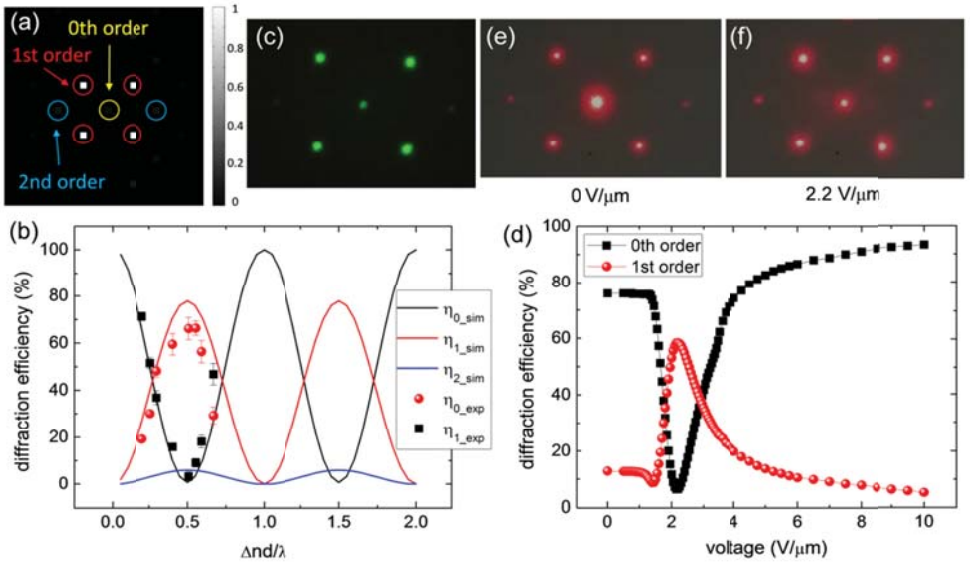

Fig. 4. Diffraction of the 2D LCPG. (a) Diffraction intensity distribution based on simulation at half-wave condition. The 0th, 1st and 2nd orders are marked respectively. (b) Diffraction efficiency of the 0th, 1st and 2nd orders with different LC phase retardation. Lines are the simulation results, and the scattered dots are from experiments. (c) Diffraction of the 2D LCPG from experiments.(d) Diffraction efficiency of the 0th and 1st orders as a function of applied electric field in a 2D LCPG cell (f = 1 kHz).All given voltages are the peak to peak values. The transmittance of a uniformly aligned LC polymer or LC cell is used as 100% efficiency reference. (e) and (f) Diffraction patterns of the 2D LCPG cell at different voltages respectively.

Optics EXPRESS

Although the LC polymer can be photoaligned on one photo-patterned substrate with desired thickness, the obtained grating is not tunable. If using a nematic LC filled into a photo-patterned cell, the effective LC birefringence Δn_{eff} can be controlled continuously by applied ac voltage, and thus the diffraction efficiency would become adjustable. Here, a nematic LC with high birefringence is used toa provide wide adjustable range in a thin cell. The electro-optical behavior of a tunable2D LCPG is shown in Figs. 4(d)-4(f). When the effective phase retardation satisfies half-wave condition, i.e. at 2.2 V/μm, the diffraction efficiency is maximized. However, the maximum diffraction efficiency is still lower than that of LC polymer film. This is caused by undefined LC pretilt angle and the small mismatch of the interference patterns recorded at the front and back substrates of the cell. The undefined LC pretilt angle causes defect lines with applied voltage and thus decreases the diffraction efficiency. The alignment mismatch causes binary grating effect, and consequently leads to higher order diffraction and non-vanishing 0th order at half-wave condition. The mismatch problem becomes more serious with thicker cell gap [34]. However, these problems could be further optimized, for example, using smaller interference polar angle and by introducing uniform pretilt angle after pattern recording [35].

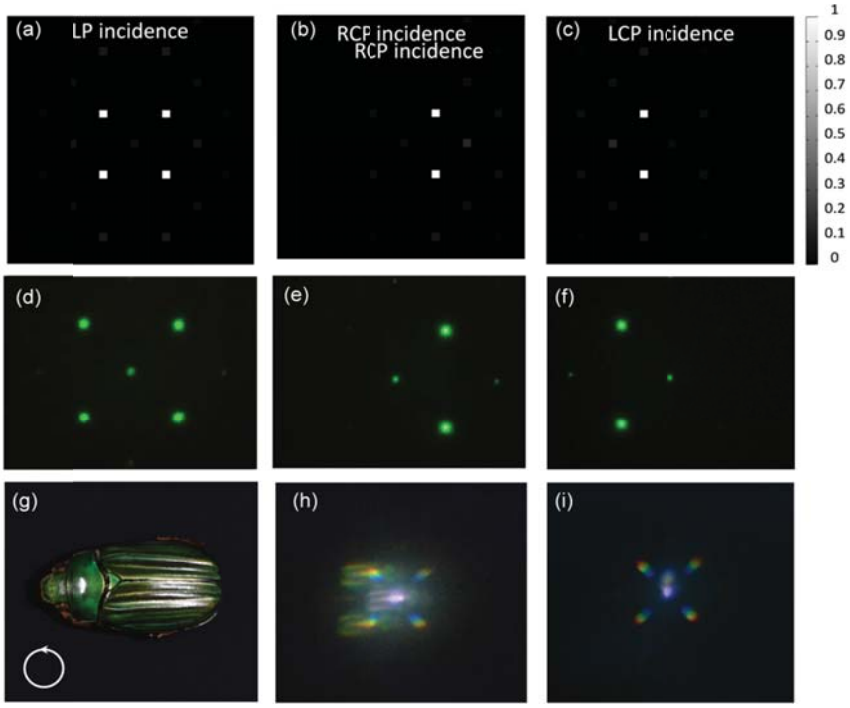

Fig. 5. Polarization selectivity of the 2D LCPG diffraction. (a-c) Simulated diffraction intensity with different polarization incidence at half-wave condition. (d-f) Experimental diffraction with different polarization incidence.(g) Photograph of a *Plusiotis gloriosa* under unpolarized light, which selectively reflects LCP light. (h) The scattered image of the beetle by a 2D LCPG. (i) Diffraction of the background stray light from the 2D LCPG without the beetle.

Polarization selectivity is expected for the 2D PG diffraction. The simulation shows that the unpolarized light or LPL will be diffracted into all the orders, while CPL is mainly diffracted into the positive or negative orders [Figs. 5(a)-5(c)]. There is a weak energy leakage on the other side with CPL incidence, but it is too weak to be considered. Experiments show consistent polarization selectivity results, as shown in Figs. 5(d)-5(f). Another example is given by the beetle *Plusiotisgloriosa* [Fig. 5(g)], which possesses a

brilliant green-striped appearance and selectively reflects LCP light [36]. The beetle is illuminated by an unpolarized white light and the reflected light is collected by a lens for imaging. A 2D LCPG is put after the lens, and the scattered image is received on the image plane, as shown in Fig. 5(h). The images of two green-striped beetles show up on the −1st order in addition to the 0th order in the middle, further confirming the polarization selectivity property of the 2D PG. The white spot in the middle and four rainbow spots on the 1st order come from the reflected stray light of the background [Fig. 5(i)], which makes the 0th order image colorless and the others with rainbow color on top.

The polarization state of the diffracted light can be monitored by the phase difference δ_{diff} between the *y*- and *x*-component of the diffracted electric vector, where RCP has $\delta_{diff} = -\pi/2$ and LCP has $\delta_{diff} = \pi/2$ [Figs. 6(a) and (b)]. When the incident light is CP, the diffracted light is pure CP with opposite helicity to the incidence. If the incident light is LP, the diffraction is the superposition of those from both LCP and RCP light. The diffraction of LP light isnear CPL due to the weak diffraction leakage, which is indicated by the small difference of δ_{diff} compared to $\pm \pi/2$ as shown in the inset of Fig. 6(b). Since the diffraction leakage is very weak, the phase difference is small and the polarization of the diffracted light is close to CPL. The helicity of the diffracted light is checked by going through a QWP and a polarizer at ± 45° based on Jones calculus. The result shows that the diffracted beams on the −1st order are RCP, and these on the + 1st order are LCP, consistent with the simulation. The ellipticity of the diffracted light can be checked by a rotating polarizer. The ellipticities of diffracted lights with both CP and LP incident lights are near 1, indicating good CPL qualities in both cases. The results confirm that the energy leakage is very weak and would not cause noticeable problems to the diffracted CPL. This property has been checked by both green and red light as shown in Figs. 7(a) and 7(b), and should be valid for all the wavelengths that are applicable for LC materials [37–39].

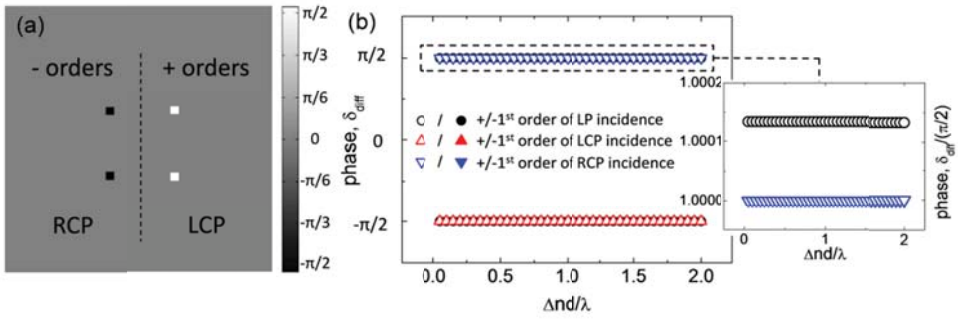

Fig. 6. The 1st order diffraction phase of the 2D LCPG. (a) The diffraction phase distribution. (b) The diffraction phases δ_{diff} with different incident polarization. The phases don't change with the LC phase retardation. Inset: normalized δ_{diff} of diffractions from CP and LP incidence.

In our design, the LPL intensity in the interference configuration is chosen to be 1/5 of the CPL. As discussed above, the polarization continuity becomes better with higher LPL intensity, which will make the 2D LCPG texture better defined and thus the experimental LC texture is more consistent with the simulation result. However, with increasing LPL intensity, the diffractions to the 0th and 2nd orders become more obvious, and the energy leakage of the 1st order to the opposite side gets stronger with CPL incidence. Therefore, the diffracted CPL quality with LPL incidence will be worse. Figures 7 (c) and 7(d) show the ellipticity measurements of the diffracted light with different introduced LPL intensity. We can see that the diffracted light becomes EPL, and the ellipticity decreases with stronger induced LPL intensity. Therefore, to incorporate LPL into the CPL interference for 2D LCPG fabrication, the LPL intensity should be chosen properly, not only considering the intensity and

Optics EXPRESS

polarization distribution of the interference field, but also taking the diffraction requirement into account. On the other hand, if CPL is induced into the other arm instead of LPL with the same intensity, the 0th order diffraction is found to be more obvious and the diffraction efficiency to the 1st order becomes lower than our design. Therefore, LPL with $I_{LPL} = I_{CPL}/5$ is chosen for 2D LCPG design after overall consideration.

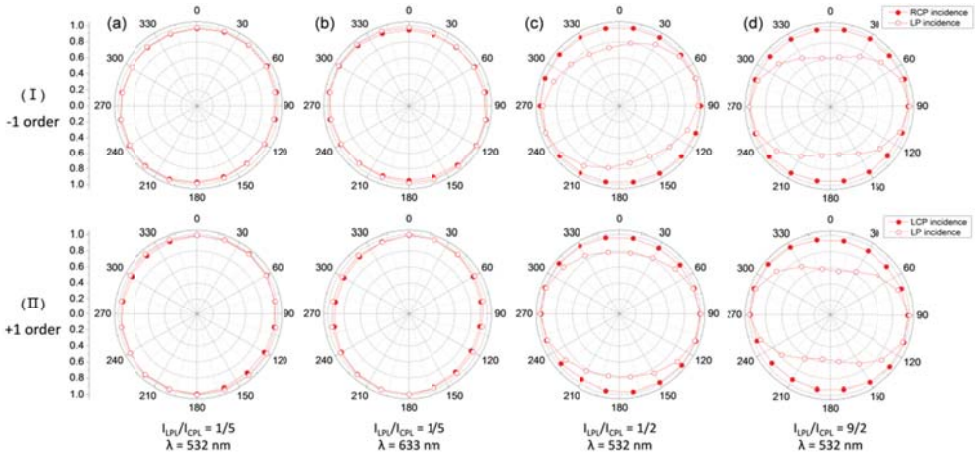

Fig. 7. Ellipticitymeasurements (normalized intensity vs. polarization angle) of the 1st order diffraction from the 2D LCPG. (a) and (b) The diffraction ellipticity measurements of the 2D LCPG fabricated with $I_{LPL} = I_{CPL}/5$ using different incident wavelengths λ = 532 nm and λ = 633 nm respectively. (c) and (d) The diffraction ellipticity measurements of the LCPG fabricated with different intensity ratio of I_{LPL}/I_{CPL}. (I) and (II) Diffractions of −1 and + 1 orders with LP (open symbols) and CP incidence (closed symbols) respectively.

4. Summary

In conclusion, a design of a 2D polarization structure through multi-beam interference is reported by introducing a LP beam into the CPL interference configuration. Since the fabrication based on LC photoalignment technology requires both full coverage of the light intensity and continuous polarization direction distribution, most multi-CPL interference fields are not qualified. The introduction of a weak LP beam may help to modify the interference field and solve these problems. In our design, we introduce a weak LP beam into a three CP beam interference configuration. The introduced LPL intensity is chosen to be 1/5 of the CPL, which not only gives well-defined LC texture, but also would not disturb the desired diffraction property of the 2D LCPG. The multi-channel diffraction of the 2D LCPG of our design keeps high efficiency, good CPL quality and polarization selective. Our proposal and design may provides another way for 2D polarization structure design and help to satisfy the critical requirement of multi-beam interference, enriching the design of 2D PGs.

Funding

National Natural Science Foundation of China (NSFC) (61875081), Shenzhen Science and Technology Innovation Council (JCYJ20180305180700747 and JCYJ20180305180611745) and National Key Research and Development Program of China administrated by the Ministry of Science and Technology of China (2016YFB0401702).

References

1. M. Stalder and M. Schadt, "Linearly polarized light with axial symmetry generated by liquid-crystal polarization converters," Opt. Lett. **21**(23), 1948–1950 (1996).
2. J. W. McIver, D. Hsieh, H. Steinberg, P. Jarillo-Herrero, and N. Gedik, "Control over topological insulator photocurrents with light polarization," Nat. Nanotechnol. **7**(2), 96–100 (2011).

Optics EXPRESS

3. P. V. Kapitanova, P. Ginzburg, F. J. Rodríguez-Fortuño, D. S. Filonov, P. M. Voroshilov, P. A. Belov, A. N. Poddubny, Y. S. Kivshar, G. A. Wurtz, and A. V. Zayats, "Photonic spin Hall effect in hyperbolic metamaterials for polarization-controlled routing of subwavelength modes," Nat. Commun. **5**(1), 3226–3233 (2014).
4. S. Stenholm, "Polarization coding of quantum information," Opt. Commun. **123**(1–3), 287–296 (1996).
5. S. Eckhardt, C. Bruzzone, D. Aastuen, and J. Ma, "3M PBS for high performance LCOS optical engine," Proc. SPIE **5002**, 106–110 (2003).
6. F. Gori, "Measuring Stokes parameters by means of a polarization grating," Opt. Lett. **24**(9), 584–586 (1999).
7. J. Tervo and J. Turunen, "Paraxial-domain diffractive elements with 100% efficiency based on polarization gratings," Opt. Lett. **25**(11), 785–786 (2000).
8. G. P. Crawford, J. N. Eakin, M. D. Radcliffe, A. Callan-Jones, and R. A. Pelcovits, "Liquid-crystal diffraction gratings using polarization holography alignment techniques," J. Appl. Phys. **98**(12), 123102 (2005).
9. V. Presnyakov, K. Asatryan, T. Galstian, and V. Chigrinov, "Optical polarization grating induced liquid crystal micro-structure using azo-dye command layer," Opt. Express **14**(22), 10558–10564 (2006).
10. M. J. Escuti and W. M. Jones, "A polarization-independent liquid crystal spatial light modulator," Proc. SPIE **6332**, 63320M (2006).
11. M. Hasegawa and Y. Taira, "Nematic homogeneous photo alignment by polyimide exposure to linearly polarized UV," J. Photopolym. Sci. Technol. **8**(2), 241–248 (1995).
12. K. Ichimura, Y. Suzuki, T. Seki, A. Hosoki, and K. Aoki, "Reversible change in alignment mode of nematic liquid crystals regulated photochemically by command surfaces modified with an azobenzene monolayer," Langmuir **4**(5), 1214–1216 (1988).
13. W. M. Gibbons, P. J. Shannon, S.-T. Sun, and B. J. Swetlin, "Surface-mediated alignment of nematic liquid crystals with polarized laser light," Nature **351**(6321), 49–50 (1991).
14. V. Chigrinov, S. Pikin, A. Verevochnikov, V. Kozenkov, M. Khazimullin, J. Ho, D. D. Huang, and H.-S. Kwok, "Diffusion model of photoaligning in azo-dye layers," Phys. Rev. E Stat. Nonlin. Soft Matter Phys. **69**(6 Pt 1), 061713 (2004).
15. C. Provenzano, P. Pagliusi, and G. Cipparrone, "Electrically tunable two-dimensional liquid crystals gratings induced by polarization holography," Opt. Express **15**(9), 5872–5878 (2007).
16. K. Kawai, M. Sakamoto, K. Noda, T. Sasaki, N. Kawatsuki, and H. Ono, "Tunable dichroic polarization beam splitter created by one-step holographic photoalignment using four-beam polarization interferometry," J. Appl. Phys. **121**(1), 013102 (2017).
17. H. Ono, A. Emoto, and N. Kawatsuki, "Anisotropic photonic grating formed in photo cross-linkable polymer liquid crystals," J. Appl. Phys. **100**(1), 013522 (2006).
18. S. P. Gorkhali, S. G. Cloutier, and G. P. Crawford, "Two-dimensional vectorial photonic crystals formed in azo-dye-doped liquid crystals," Opt. Lett. **31**(22), 3336–3338 (2006).
19. U. Ruiz, C. Provenzano, P. Pagliusi, and G. Cipparrone, "Pure two-dimensional polarization patterns for holographic recording," Opt. Lett. **37**(3), 311–313 (2012).
20. U. Ruiz, P. Pagliusi, C. Provenzano, V. P. Shibaev, and G. Cipparrone, "Supramolecular chiral structures: smart polymer organization guided by 2D polarization light patterns," Adv. Funct. Mater. **22**(14), 2964–2970 (2012).
21. M. Campbell, N. D. Sharp, and T. M. Harrison, "Fabrication of photonic crystals for the visible spectrum by holographic lithography" Nature ||London|**404**, 53–56 ||2000|.
22. Y. J. Liu and X. W. Sun, "Electrically tunable two-dimensional holographic photonic crystal fabricated by a single diffractive element," Appl. Phys. Lett. **89**(17), 171101 (2006).
23. D. Luo, X. W. Sun, H. T. Dai, Y. J. Liu, H. Z. Yang, and W. Ji, "Two-directional lasing from adye-doped two-dimensional hexagonal photonic crystal made of holographic polymer-dispersed liquid crystals," Appl. Phys. Lett. **95**(15), 151115 (2009).
24. Y. Shi, Y. J. Liu, F. Song, V. G. Chigrinov, H. S. Kwok, M. Hu, D. Luo, and X. W. Sun, "Photoalignment-induced two-dimensional liquid crystal polarization structure via multi-beam polarization interferometry," Opt. Express **26**(6), 7683–7692 (2018).
25. P. G. de Gennes and J. Prost, *The Physics of Liquid Crystals* (Oxford University, 1995).
26. M. Born and E. Wolf, *Principles of Optics: Electromagnetic Theory of Propagation, Interference and Diffraction of Light* (Cambridge University, 1999).
27. V. Chigrinov, H. S. Kwok, H. Takada, and H. Takatsu, "Photo-aligning by azo-dyes: physics and applications," Liquid Crystals Today **14**(4), 1–15 (2005).
28. J. Li, J. Li, M. Hu, Z. Che, L. Mo, X. Yang, Z. An, and L. Zhang, "The effect of locations of triple bond at terphenyl skeleton on the properties of isothiocyanate liquid crystals," Liq. Cryst. **44**(9), 1374–1383 (2017).
29. Z. Sekkat and W. Knoll, *Photoreactive Organic Thin Films* (Academic, 2002).
30. L. Tan, J. Y. Ho, and H.-S. Kwok, "22.1: Binary alignment pattern induced by single step exposure of laser beam polarization interference," SID Dig. **43**(1), 286–288 (2012).
31. V. G. Chigrinov, *Liquid Crystal Photonics* (Nova Science Publishers Inc.: New York, 2014).
32. H. Wu, W. Hu, H.-C. Hu, X.-W. Lin, G. Zhu, J.-W. Choi, V. Chigrinov, and Y.-Q. Lu, "Arbitrary photo-patterning in liquid crystal alignments using DMD based lithography system," Opt. Express **20**(15), 16684–16689 (2012).
33. Y. Shi, C. Zhao, J. Y.-L. Ho, V. V. Vashchenko, A. K. Srivastava, V. G. Chigrinov, H.-S. Kwok, F. Song, and D. Luo, "Exotic property of azobenzenesulfonic photoalignment material based on relative humidity," Langmuir **33**(16), 3968–3974 (2017).

Optics EXPRESS

34. V. Presnyakov, K. Asatryan, T. Galstian, and V. Chigrinov, "Optical polarization grating induced liquid crystal micro-structure using azo-dye command layer," Opt. Express **14**(22), 10558–10564 (2006).
35. V. G. Chigrinov, V. M. Kozenkov, and H. S. Kwok, *Photoalignment of Liquid Crystalline Materials: Physics and Applications* (Wiley Publishing, 2008).
36. V. Sharma, M. Crne, J. O. Park, and M. Srinivasarao, "Structural origin of circularly polarized iridescence in jeweled beetles," Science **325**(5939), 449–451 (2009).
37. S.-T. Wu, "Birefringence dispersions of liquid crystals," Phys. Rev. A Gen. Phys. **33**(2), 1270–1274 (1986).
38. H. Park, E. P. J. Parrott, F. Fan, M. Lim, H. Han, V. G. Chigrinov, and E. Pickwell-MacPherson, "Evaluating liquid crystal properties for use in terahertz devices," Opt. Express **20**(11), 11899–11905 (2012).
39. F. Yang and J. R. Sambles, "Determination of the microwave permittivities of nematic liquid crystals using a single metallic slit technique," Appl. Phys. Lett. **81**(11), 2047–2049 (2002).